ISSN 1349-1113
JAXA-RR-06-012E

JAXA Research and Development Report

Non-contact Thermophysical Property Measurements of Liquid and Supercooled Osmium

Takehiko ISHIKAWA, Paul-François PARADIS
and Noriyuki KOIKE

March 2007

Japan Aerospace Exploration Agency

Non-contact Thermophysical Property Measurements of Liquid and Supercooled Osmium

Takehiko ISHIKAWA[*1], Paul-François PARADIS[*1] and Noriyuki KOIKE[*2]

Abstract: In a first step of a comprehensive study of the macroscopic and microscopic properties and structure of osmium, solid samples were successfully levitated, melted, deeply undercooled and re-solidified under vacuum. Using non-contact diagnostic methods, several properties of equilibrium and non-equilibrium liquid osmium were measured. Over the 2670-3380 K temperature range, the density could be expressed as $\rho(T)=1.91 \times 10^4 - 1.16\ (T-T_m)$ kg·m^{-3}, where T_m is the melting temperature (T_m=3306 K). Similarly, the surface tension and the viscosity measurement data could be fitted respectively as $\gamma(T) = 2.48 \times 10^3 - 0.34\ (T-T_m)$ mN·m^{-1} and $\eta(T) = 0.00167 \exp[2.2 \times 10^5/(RT)]$ mPa·s over the 3230-3605 K temperature interval.

Keywords: osmium, liquid, density, surface tension, viscosity

1. INTRODUCTION

The report that metallic osmium has a lower compressibility than covalently bonded diamond[1] has renewed the interest in this elemental metal, in particular in view of synthesizing new and harder materials. This triggered several basic studies of its high-pressure behavior,[2] its structural phase transitions, its mechanical properties,[3] and its electronic and crystalline structure.[4] However, to synthesize novel osmium-based multi-function alloys from solidification of non-equilibrium (e.g., undercooled) liquids, fundamental knowledge in areas of properties and structure is needed and macroscopic and microscopic characterization of its liquid phases are required. However, although non-equilibrium states influence the microstructure upon solidification,[5] little or no attention has been given so far to this elemental metal.

In discussing the nature and behavior of liquids, density, surface tension, and viscosity are fundamental quantities needed to describe the radial distribution function, diffusion phenomena, gas adsorption, nucleation, and rise of bubbles in melts.[6] Moreover, knowledge of their temperature dependence is of critical importance to understand solidification and convection. From a practical aspect, these properties provide essential information to optimize industrial processes.

However, no direct density or viscosity measurements of osmium were reported for its liquid phase (surface tension data limited to the melting point). This is attributable to its elevated melting temperature (3306 K),[7] the highest among the platinum group metals, the toxicity problems with oxides, its high vapor pressure, and the risks of contamination. To fill this void and to check the technical feasibility of maintaining a sample of Os in its liquid phase at a given temperature over long time scales (minutes-hours), experiments were undertaken in this study using a vacuum electrostatic levitation furnace.[8,9] In addition of supplying property data over a large temperature range, these experiments would make possible to investigate the atomic structure by synchrotron radiation scattering experiments and to conduct systematic solidification studies. In this report, the density, surface tension, and viscosity measurements of liquid Os are presented over a wide temperature range, including the undercooled region.

＊1 Japan Aerospace Exploration Agency, 2-1-1 Sengen, Tsukuba, Ibaraki, Japan 305-8505.
＊2 Chiba Institute of Technology, 2-17-1 Tsudanuma, Narashino, Chiba, Japan.

2. EXPERIMENTAL SETUP AND PROCEDURES

2.1. Electrostatic Levitation Furnace

The measurements were made using an electrostatic levitator (Fig. 1),[10,11] which consisted of a chamber evacuated to a ~10^{-5} Pa vacuum level before processing was initiated. The chamber housed a sample charged by electronic emission and levitated between electrodes via a feedback loop. The two disk electrodes were used for the vertical position control whereas four spherical electrodes were dedicated to horizontal control.[12] The positioning control relied on two sets of orthogonally arranged He-Ne lasers and the associated position detectors. The three dimensional sample position information was fed to a computer that generated and sent appropriate x, y, and z position control signals to high voltage amplifiers so that a prefixed sample position can be maintained. The lower electrode was surrounded by four coils that generated a rotating magnetic field that was used for rotation control.[13] Specimens were prepared by arc melting 99.8 % mass purity osmium powder (Nilaco Corp., Japan) into spheroids with diameters of *ca.* 1.5 mm.

Three laser beams were used for sample heating (Fig. 1). The beam of one CO_2 laser (10.6 μm emission) was sent directly to the sample whereas that from another CO_2 laser was divided into two beams such that the three focused beams in a same plane, separated by 120 degrees, hit the specimen. This configuration provided temperature homogeneity, sample position stability, and helped to control sample rotation.

The radiance temperature was measured with a single-color pyrometer (0.90 μm, 120 Hz acquisition rate) covering a 900 to 3800 K interval. The temperature was calibrated to true temperature using the melting plateau of the sample (T_m = 3306 K).

The sample was observed by three charge-coupled-device (CCD) cameras. One color camera offered a view of both the electrodes and the sample whereas two black and white high-resolution cameras (camera-1 and camera-2), located at right angles from each other and equipped with telephoto objectives, provided magnified views of the sample for density measurements. This also helped to monitor the sample position in the horizontal plane and to align the heating laser beams to minimize photon-induced horizontal sample motion and sample rotation.[14]

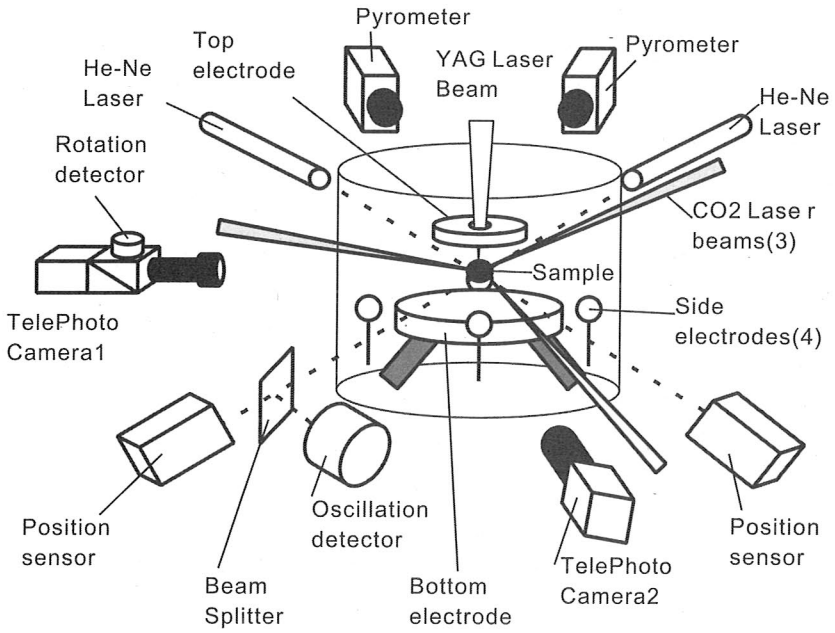

Fig. 1 Schematic view of the electrostatic levitation furnace and its diagnostic apparatus.

2.2. Thermophysical Property Determination

Density measurements were carried out using a UV imaging technique described in detail elsewhere.[9,15] First, a solid sample was levitated and rotation about the vertical-axis was induced by a rotating magnetic field. The rotation rate of the solid sample was measured by a rotation detector, which monitors the intensity of He-Ne lasers reflected from the uneven sample surface.[13] When the rotation rate

reached 10 Hz, the rotating magnetic field was turned off. All CO_2 laser beams were directed in such a way to minimize photon-induced rotation during the sample heating. Once a levitated sample was melted (ca. 1.5 mm diameter, nearly 30 mg), it became spherical due to surface tension and the distribution of surface charge. If the shape of a molten sample departed from that of a sphere (due to excessive rotation), a counter torque was applied by the magnetic field to restore the spherical shape. The controlled sample rotation not only improved the temperature homogeneity of the sample,[16] but also prevented precession and ensured the axi-symmetry of the sample along the vertical axis.

Images at the rate of 30 frames/s and temperature data were simultaneously recorded as a function of time. All laser beams were then blocked with mechanical shutters allowing the sample to cool radiatively. After the experiment, the video images from one high-resolution camera were digitized. Since the sample was axi-symmetric, the sample volume could be calculated from each image. The recorded images were calibrated by levitating a stainless sphere with a precisely known radius under identical experimental conditions. The images were then matched with the thermal history of the sample (Fig. 2). Because the mass of the sample was known, the density could be determined as a function of temperature. Although the sample evaporated as evidenced by a change in radius during long levitation periods (hours), the density experiments lasted only a few minutes, for which the melting temperature was exceeded for only a few seconds (Fig. 2). Therefore, the effect on density was negligible.

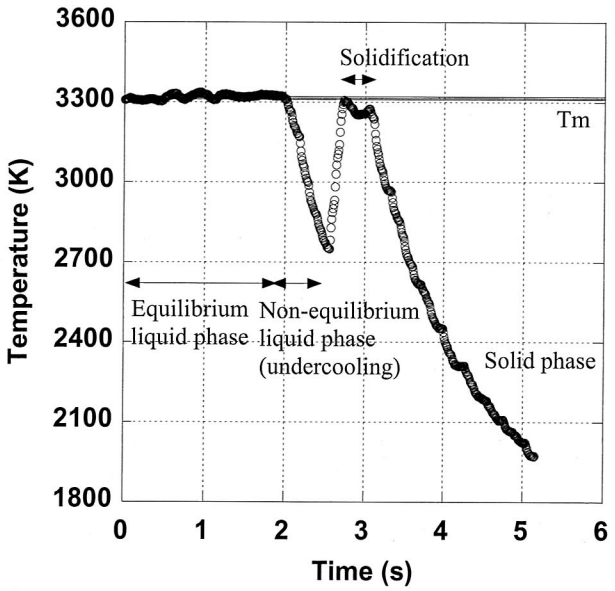

Fig. 2 Radiative temperature profile for an osmium sample showing undercooling and recalescence.

The surface tension and viscosity were determined by the oscillating drop method.[17] In this method, a solid sample was first levitated, rotated around 10 Hz, heated, melted, and brought to a selected temperature. Then, a $P_2(\cos\theta)$-mode drop oscillation was induced to the sample by superimposing a small sinusoidal electric field on the levitation field. One of the positioning He-Ne laser beams was divided by a beam splitter and lead to an oscillation detector, which consisted of a power detector and a vertical slit. The shadow of the levitated sample was projected on this detector and variation of the vertical diameter of the sample was translated to an electrical signal.[18] The transient signal that followed the termination of the excitation field was detected and analyzed using a custom-made program. This was done several times at a given temperature and repeated for several temperatures. Using the characteristic oscillation frequency ω_c of the signal, which was calculated by a fast Fourier transform (FFT) analysis and then corrected for non uniform surface charge distribution, the surface tension γ can be determined from:[18]

$$\omega_c^{\,2} = \left(\frac{8\gamma}{\rho r_0^{\,3}}\right) Y, \tag{1}$$

where r_0 is the radius of the sample, ρ is the density, and Y is the correction factor that depends on the drop charge, the permittivity of vacuum, and the applied electric field.[19,20] Similarly, using the decay time τ given by the same signal, the viscosity η can be determined by

$$\eta = \frac{\rho r_0^2}{5\tau} \cdot {}^{21)} \tag{2}$$

During the experiments, the video images from a high-resolution camera were recorded. After the experiment, each value of the radius at each oscillation was obtained by image analysis. This procedure eliminated the measurement error due to sample evaporation. Moreover, the aspect ratio of the sample (ratio between the horizontal and vertical radii) was also calculated to evaluate the experimental error induced by sample rotation.

2.3. Experimental Uncertainties

The experimental uncertainty for density measurements was derived from the respective uncertainty measurements for the mass and volume of samples. Because the uncertainty in mass was 0.1 mg while a typical osmium sample mass was 30 mg, the uncertainty can be estimated to be around 0.3 %. The uncertainty of volume ($\Delta V/V$) can be calculated by

$$\frac{\Delta V}{V} = \frac{3\Delta r_0}{r_0} \tag{3}$$

where Δr_0 is the uncertainty in radius measurement by the image analysis[15]. In our experiment, the average value of Δr_0 was around 1 pixel, while r_0 was 160 pixels. Therefore, $\Delta V/V$ can be estimated to be around 1.9 %, and the overall uncertainty of density measurement ($\Delta\rho/\rho$) was estimated to be about 2 %.

Based on equation (1), the uncertainty in surface tension measurement was mainly determined by those of ρ, r_0, and ω_c. As described earlier, the uncertainty of ρ and r_0 were 2 % and 0.65 %, respectively. The uncertainty of ω_c induced by the FFT analysis was negligibly small (0.4 %) and evaluated by considering the transformation error (less than 1 Hz) and the typical characteristic oscillation frequency (around 250 Hz). As a result, the uncertainty of surface tension measurements ($\Delta\gamma/\gamma$) can be estimated to be around 3 % by the following equation:

$$\frac{\Delta\gamma}{\gamma} \approx \sqrt{\left(\frac{\Delta\rho}{\rho}\right)^2 + \left(\frac{3\Delta r_0}{r_0}\right)^2 + \left(\frac{\Delta\omega_c}{\omega_c}\right)^2} \,. \tag{4}$$

Similarly, the uncertainty of viscosity measurement can be estimated by the uncertainties of ρ, r_0, and τ. The uncertainty of the decay time $\Delta\tau$ was estimated to be about 15 %, which was due mainly to the sample motion with respect to the detector during drop oscillation. This determined the overall uncertainty of viscosity.

3. RESULTS AND DISCUSSIONS

3.1. Density

The density measurements of liquid osmium, taken over the 2670 to 3380 K temperature range and extending into the undercooled region by around 635 K, are shown in Fig. 3. Several data points in Fig. 3 are shown with 2 % experimental error bars. The density, like that of other pure metals, exhibits a linear behavior as a function of temperature and can be fitted by the following relationship with a confidence interval of 95 %:

$$\rho(T) = (19.1 \pm 0.4) \times 10^3 - (1.16 \pm 0.11)\,(T - T_m)\ (\mathrm{kg \cdot m^{-3}}) \qquad (2670 \text{ to } 3380\ \mathrm{K}) \tag{5}$$

where T_m is the melting temperature (3306 K). The volume variation $V(T)$ of the molten state, normalized with the volume at the melting temperature V_m, was derived from eq. (5), and can be expressed by

$$V(T)/V_m = 1 + 6.1 \times 10^{-5}\,(T - T_m) \tag{6}$$

where 6.1×10^{-5} ($\mathrm{K^{-1}}$) represents the volume expansion coefficient at the melting temperature (β_m).

Although no experimental data have been reported, our density data agreed well with calculated values. As for the density at the melt-

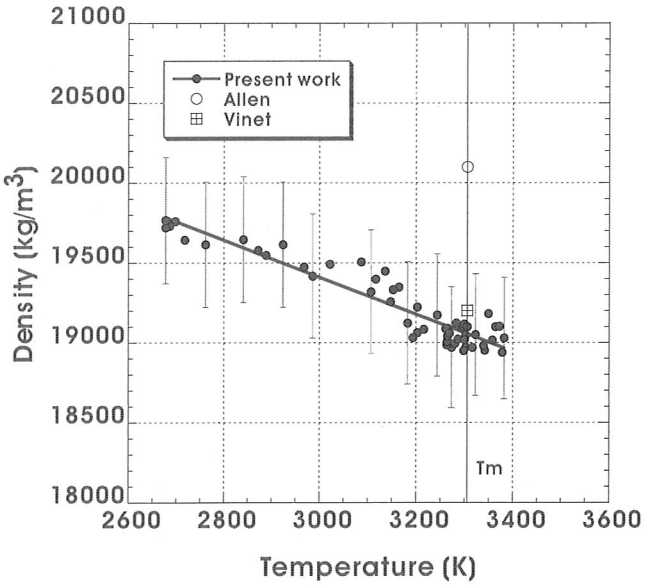

Fig. 3 Density of liquid osmium versus temperature

ing temperature (ρ_m), our value was, within the experimental uncertainties, identical to the calculation by Vinet *et al.*[22] from surface tension data and less than 5% lower than that calculated by Allen[23] from room-temperature specific volumes increased for cubical thermal expansion to the melting point.

No temperature coefficient data were reported but our thermal expansion coefficient of osmium was similar to those of other transition metals. A simple relationship between the temperature dependence of the density of liquid metals and their boiling temperatures (T_b) was proposed by Steinberg[24]. He collected liquid density data at the melting point and the temperature dependence of liquid density for 44 elements and found the following empirical relations

$$-\frac{d\rho}{dT} \propto \frac{\rho_{00}}{T_b} \tag{7}$$

where ρ_{00} was the virtual density of the liquid at 0 K determined by extrapolation from ρ_m and T_m with:

$$\rho_{00} = \rho_m - \frac{d\rho}{dT} T_m \tag{8}$$

Figure 4 illustrates the correlation of $-d\rho/dT$ with ρ_{00}/T_b. In his study, Most of metal elements followed the correlation. In Fig.4, our measured data of refractory metals[25-28] including that of osmium was also plotted. Our osmium data (-1.16 $kg \cdot m^{-3} \cdot K^{-1}$), as well as those for other refractory metals, showed a good agreement with Steinberg's relation.

3.2. Surface Tension

Figure 5 depicts the results for the surface tension of osmium. Several data points in Fig. 5 have the 3 % error bars indicating the experimental uncertainty described in 2.3. The surface tension data, measured over the 3230 to 3605 K temperature range and extending into the undercooled region by 75 K, can be expressed by

$$\gamma(T) = 2.48 \times 10^3 - 0.34\,(T - T_m)\ (10^{-3} N \cdot m^{-1}) \quad (3230 \text{ to } 3605 \text{ K}). \tag{9}$$

When the experimental uncertainties were considered, our datum at the melting temperature was identical to that measured by Allen[23] with the pendant drop technique in vacuum and slightly higher than 3% compared to that obtained by Vinet *et al.*[22] with the drop weight technique under very high vacuum.

No other experimental data were reported for the temperature coefficient of the surface tension. Our value was very close to that esti-

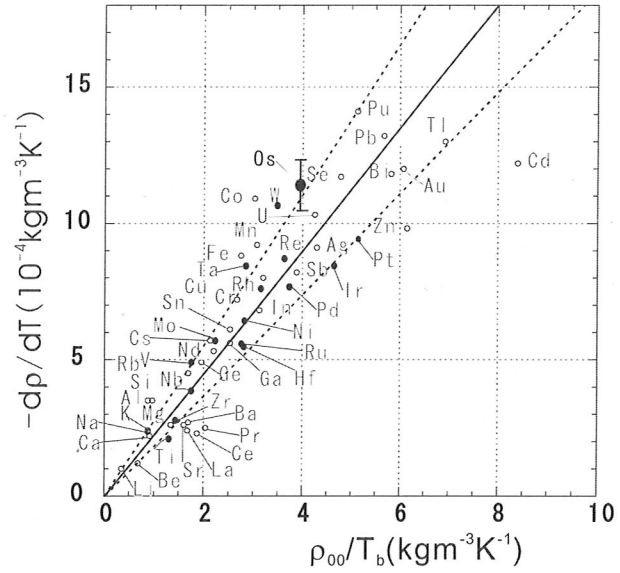

Fig. 4 Correlation of $d\rho/dT$ with ρ_{00}/T_b for elements. Open and black circles represent data from Ref. 6 and refractory metals measured by electrostatic levitator, respectively. Os data in present work is plotted with a big black circle. The solid line is the best fit to the data and the dashed lines represent the 20% error cone from Ref.24.

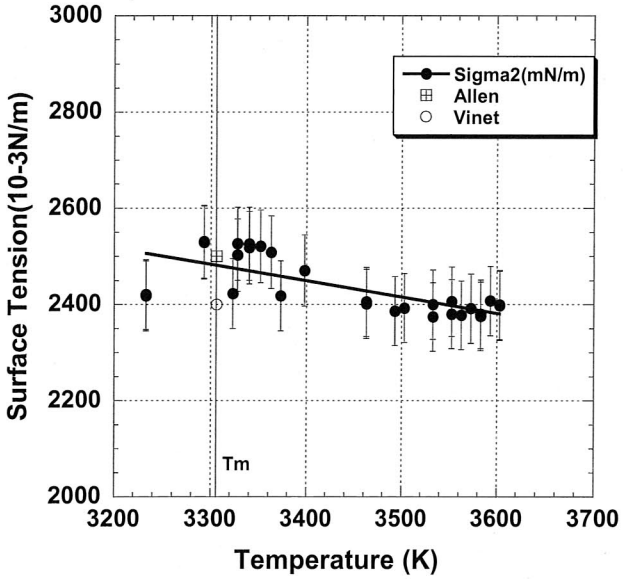

Fig. 5 Surface tension of osmium versus temperature.

mated by Allen (-0.33 x 10^{-3} N·m^{-1}·K^{-1})[29] with the following equation;

$$\frac{d\gamma}{dT} = \frac{\gamma}{T_c - T}\left[\frac{2(Tc - T)}{3\rho}\frac{d\rho}{dT} - 1\right] \tag{10}$$

where T_c is the critical temperature, but over 46% lower than that calculated by Morita *et al.*[30]

Kasama *et al.*[31] proposed an empirical equation based on a physical model. Based on this model, surface tension and its temperature dependence can be expressed as

$$\gamma = \frac{1}{2}\frac{\pi^2 C^2 \delta^2 T_m}{N_A M^{2/3}}\left(\frac{\rho}{\rho_m}\right)^{2/3}\left\{(\alpha+1)\rho^{1/3}-\rho_m^{1/3}\right\}^2$$

$$\frac{d\gamma}{dT} = -\frac{1}{3}\frac{\pi^2 C^2}{N_A}\frac{T_m \Lambda \delta^2}{M^{2/3}}\left\{2(\alpha+1)^2\rho^{1/3}\rho_m^{2/3}+\rho^{-1/3}-3(1+\alpha)\rho_m^{-1/3}\right\} \quad (11)$$

where N_A was Avogadro's number, M was the atomic number, and Λ was the temperature dependence of density ($-d\rho/dT$). In addition, a constant C, derived from Lindemann's theory of melting, ranged from 2.8 x 10^{12} to 3.1 x 10^{12}, δ, the ratio between the characteristic vibration frequency in the liquid phase and the solid phase was estimated to be around 0.5, and α, a constant indicating the distance where an attractive force by an atom was effective, ranged from 0.45 to 0.65.

At the melting temperature, the temperature coefficient of the surface tension could be calculated by

$$\frac{d\gamma}{dT} = -\frac{1}{3}\frac{\pi^2 C^2}{N_A}\frac{T_m \Lambda \delta^2}{M^{2/3}}\rho_m^{-1/3}\left(2\alpha^2+\alpha\right) \quad (12)$$

In this formula, the uncertainties of the constants (C, α, and δ) seriously affected the temperature dependence of the surface tension. Two of those constants could be eliminated by combining equations (11) and (12), and the temperature coefficient of the surface tension could be determined as

$$\frac{d\gamma}{dT} = -\frac{2}{3}\frac{\Lambda\gamma_m}{\rho_m}\frac{2\alpha+1}{\alpha} = K\frac{\Lambda\gamma_m}{\rho_m} = K\gamma_m\beta_m$$

$$K \equiv \frac{-2(2\alpha+1)}{3\alpha} \quad (13)$$

and this equation suggested that the temperature dependence of the surface tension was proportional to the product of the surface tension at the melting temperature and the thermal expansion coefficient.

Validity of this formula for liquid metals was checked by using literature data[29,32,33] and our measurements obtained with the electrostatic levitator (ESL)[34,35]. Results are shown in figure 6.

Literature data of alkaline metals showed good agreements with the equation (13), while those of transition metals scattered, some of

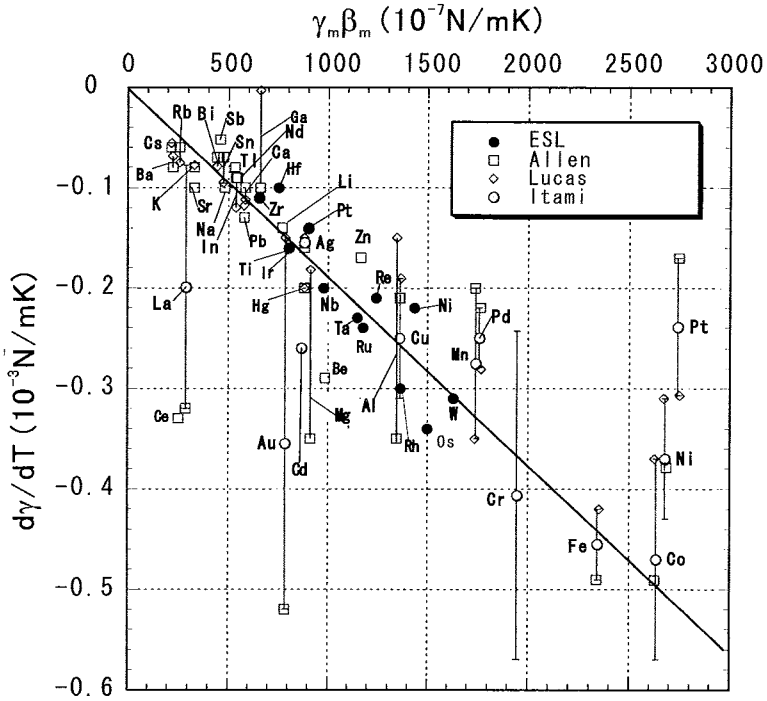

Fig.6 Correlation between $\gamma_m\beta_m$ and $d\gamma/dT$

them being far from the relation. On the other hand, measured data of refractory metals with ESL showed the same tendency as the alkaline metals. Based on the ESL results, temperature dependence of surface tension of metal elements could be estimated if the surface tension at their melting temperature and thermal expansion coefficient were known.

3.3. Viscosity

Figure 7 illustrates our data that can be fitted by the following Arrhenius function:

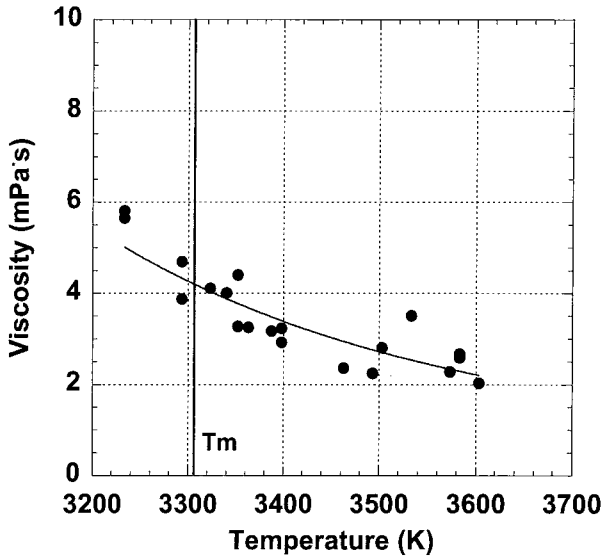

Fig. 7. Viscosity of osmium versus temperature.

$$\eta(T) = 0.00167\exp[2.2 \times 10^5/(RT)]\ (10^{-3}\text{Pa·s}) \qquad (3230 \text{ to } 3605 \text{ K}), \tag{14}$$

where R, the gas constant, is equal to 8.31 $\text{J·mol}^{-1}\text{·K}^{-1}$. The scatter observed in the data is mainly due to the motion of the sample with respect to the oscillation detector. No reference value was found in the literature.

4. CONCLUSIONS

The density, the surface tension, and the viscosity of liquid osmium were measured with an electrostatic levitator and the data were reported. The containerless processing and non-contact measurement techniques eliminated contamination from the crucibles as well as suppressed nucleation at the melting temperature. This enabled the measurement of the thermophysical properties over wide temperature ranges, including the undercooled state. Measurements over wide temperature ranges could help determine the temperature dependence of each property with high accuracies. Our results of the temperature dependence of density and surface tension agreed well with the empirical equations provided by Steinberg and Allen.

ACKNOWLEDGMENTS

Special thanks to Mr. Y. Watanabe (A.E.S. Co. ltd.) and Mr. R. Ishikawa (Tokyo University) for help in some experiments. This work was supported by a Grant-in-Aid for Scientific Research (B) from the Japan Society for the Promotion of Science.

REFERENCES

1) H. Cynn, J.E. Klepeis, C.-S. Yoo, and D.A. Young, *Phys. Rev. Lett.* **88** (2002), 135701.
2) M. Hebbache and M. Zemzemi, *Phys. Rev.* **B 70** (2004), 224107.
3) K. Takemura, *Phys. Rev.* **B 70** (2004), 012101.
4) Y. Ma, T. Cui, L. Zhang, Y. Xie, G. Zou, J.S. Tse, X. Gao, and D.D. Klug, *Phys. Rev.* **B 72** (2005), 174103.
5) F. Spaepen, *Science* **235** (1987), 1010.
6) T. Iida and R. I. L. Guthrie: *The Physical Properties of Liquid Metals*, (Clarendon Press, Oxford 1988).
7) D. R. Lide and H. P. R. Frederikse: *CRC Handbook of Chemistry and Physics*, (CRC Press, Boca Raton, Florida, 1997) 78th ed.
8) P.-F. Paradis, T. Ishikawa, and S. Yoda, *Appl. Phys. Lett.* **83** (2003), 4047.
9) T. Ishikawa, P.-F. Paradis, and S. Yoda: *Rev. Sci. Instrum.* **72** (2001), 2490.
10) P.-F. Paradis, T. Ishikawa, and S. Yoda: ESA **SP-454** (2001) 993.
11) T. Ishikawa, P.-F. Paradis, and S. Yoda, *J. Jpn. Soc. Microg. Appl.* **18** 106 (2001).
12) W. -K. Rhim, S. -K. Chung, D. Barber, K.-F. Man, G. Gutt, A. A. Rulison, and R. E. Spjut, *Rev. Sci. Instrum.* **64** (1993) 2961.
13) W.-K. Rhim and T. Ishikawa, *Rev. Sci. Instrum.* **69** (1998) 3628.
14) W.-K. Rhim and P.-F. Paradis, *Rev. Sci. Instrum.***70** (1999) 4652.
15) S.-K. Chung, D. B. Thiessen, and W.-K. Rhim, *Rev. Sci. Instrum.* **67** (1996) 3175.
16) R.W.Hyers, *Meas. Sci. Technol.* **16** (2005), 394.
17) Lord Rayleigh, *Proc. R. Soc. London* **29** (1879), 71.
18) W.-K. Rhim, K. Ohsaka, and P.-F. Paradis, *Rev. Sci. Instrum.* **70** (1999), 2996.
19) Lord Rayleigh, *Philos. Mag.* **14** (1882), 184.
20) J. Q. Feng and K. V. Beard, *Proc. R. Soc. London* **A 430** (1990), 133.
21) H. Lamb, *Hydrodynamics* (Cambridge University Press, 1932) 6th ed., 473.
22) B. Vinet, L. Magnusson, H. Fredriksson, and J.-P. Desre, *J. Coll. Interf. Sci,* **255** (2002), 363.
23) B. C. Allen, Trans. AIME **227** (1963), 1175.
24) D. J. Steinberg, *Metallurgical Transactions* **5** (1974), 1341.
25) T. Ishikawa, P.-F. Paradis, T. Itami, and S. Yoda, *Meas.Sci. Technol.* **16** (2005), 443.
26) T.Ishikawa and P.-F. Paradis, *Journal of Electronic Materials,* **34** (2005), 1526.
27) P. -F. Paradis, T. Ishikawa, R. Fujii, and S. Yoda, *Appl. Phys. Lett.* **86** (2005), 41901.
28) T. Ishikawa, P.-F. Paradis, and N. Koike, *JJAP* **45** (2006), 1719.
29) B. C. Allen: *Liquid Metals Chemistry and Physics,*ed. S. Z. Beer (Marcel Dekker, 1972),Chap. 4, 188.
30) Z. Morita, T. Iida, A. Kasama, *Bull Japan Inst Metals* **15** (1976), 743.
31) A. Kasama, T. Iida, and Z. Morita, *J. Japan Inst. Metals*, **40** (1976), 1030.
32) L. D. Lucas, *Tech l'Ing.*, 7, Form. M65 (1984).
33) T. Itami, in *Condensed Matter Disordered Solids,* ed. S. K. Srivastava and N. H. March (World Scientific. 1995), Chap.3.
34) T. Ishikawa, P.-F. Paradis, T. Itami, and S. Yoda, *JAXA Research and Development Report*, JAXA-RR-04-024E (2005).
35) T. Ishikawa, P.-F. Paradis, and N. Koike, *JAXA Research and Development Report*, JAXA-RR-05-015E (2006).

JAXA Research and Development Report JAXA-RR-06-012E

Date of Issue: March 31, 2007
Edited and Published by: Japan Aerospace Exploration Agency
7-44-1 Jindaiji-higashimachi, Chofu-shi, Tokyo 182-8522, Japan
URL: http://www.jaxa.jp/
Printed by: TOKYO PRESS Co., Ltd.

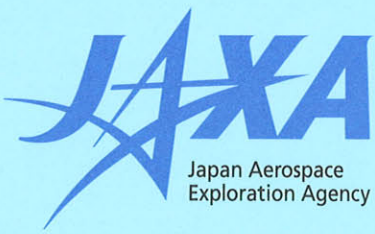

Printed on Recycle Paper